



**Michigan  
Technological  
University**

Michigan Technological University  
**Digital Commons @ Michigan Tech**

---

Department of Materials Science and  
Engineering Publications

Department of Materials Science and  
Engineering

---

1-22-2015

## Effect of Ambient Combinations of Argon, Oxygen, and Hydrogen on the Properties of DC Magnetron Sputtered Indium Tin Oxide Films

M. Marikkannan  
*Madurai Kamaraj University*

M. Subramanian  
*Nagoya Institute of Technology*

J. Mayandi  
*Madurai Kamaraj University*

M. Tanemura  
*Nagoya Institute of Technology*

V. Vishnukanthan  
*Centre for Materials Science and Nanotechnology*

*See next page for additional authors*

Follow this and additional works at: [https://digitalcommons.mtu.edu/materials\\_fp](https://digitalcommons.mtu.edu/materials_fp)

---

### Recommended Citation

Marikkannan, M., Subramanian, M., Mayandi, J., Tanemura, M., Vishnukanthan, V., & Pearce, Joshua M. (2015). Effect of ambient combinations of argon, oxygen, and hydrogen on the properties of DC magnetron sputtered indium tin oxide films. *AIP Advances*, 5(1). [http://digitalcommons.mtu.edu/materials\\_fp/5](http://digitalcommons.mtu.edu/materials_fp/5)

Follow this and additional works at: [https://digitalcommons.mtu.edu/materials\\_fp](https://digitalcommons.mtu.edu/materials_fp)

---

## Authors

M. Marikkannan, M. Subramanian, J. Mayandi, M. Tanemura, V. Vishnukanthan, and Joshua M. Pearce



## Effect of ambient combinations of argon, oxygen, and hydrogen on the properties of DC magnetron sputtered indium tin oxide films

M. Marikkannan, M. Subramanian, J. Mayandi, M. Tanemura, V. Vishnukanthan, and J. M. Pearce

Citation: [AIP Advances](#) **5**, 017128 (2015); doi: 10.1063/1.4906566

View online: <http://dx.doi.org/10.1063/1.4906566>

View Table of Contents: <http://scitation.aip.org/content/aip/journal/adva/5/1?ver=pdfcov>

Published by the [AIP Publishing](#)

---

### Articles you may be interested in

[The post-growth effect on the properties of Cu<sub>2</sub>ZnSnS<sub>4</sub> thin films](#)

[J. Renewable Sustainable Energy](#) **7**, 011203 (2015); 10.1063/1.4908063

[The effect of hydrogen on Cu 3 N thin films deposited by radio frequency magnetron sputtering](#)

[J. Appl. Phys.](#) **100**, 103509 (2006); 10.1063/1.2388123

[Characterization of the physical and electrical properties of Indium tin oxide on polyethylene naphthalate](#)

[J. Appl. Phys.](#) **98**, 083705 (2005); 10.1063/1.2106013

[p-type semiconducting Cu 2 O–CoO thin films prepared by magnetron sputtering](#)

[J. Vac. Sci. Technol. A](#) **21**, 1336 (2003); 10.1116/1.1580491

[Properties of dc magnetron sputtered indium tin oxide films on polymeric substrates at room temperature](#)

[J. Appl. Phys.](#) **89**, 5199 (2001); 10.1063/1.1357470

---

**Computing**  
SCIENCE & ENGINEERING

AIP's JOURNAL OF COMPUTATIONAL TOOLS AND METHODS.  
**AVAILABLE AT MOST LIBRARIES.**

## Effect of ambient combinations of argon, oxygen, and hydrogen on the properties of DC magnetron sputtered indium tin oxide films

M. Marikkannan,<sup>1</sup> M. Subramanian,<sup>2</sup> J. Mayandi,<sup>1,3,a</sup> M. Tanemura,<sup>2</sup>  
 V. Vishnukanthan,<sup>4</sup> and J. M. Pearce<sup>3,5,a</sup>

<sup>1</sup>*Department of Materials Science, School of Chemistry, Madurai Kamaraj University, Tamil Nadu, Madurai-625021, India*

<sup>2</sup>*Department of Frontier Materials, Graduate School of Engineering, Nagoya Institute of Technology, Gokiso-cho, Showa-ku, Nagoya 466-8555, Japan*

<sup>3</sup>*Department of Materials Science & Engineering, Michigan Technological University, USA*

<sup>4</sup>*Department of Physics, Centre for Materials Science and Nanotechnology, University of Oslo, P.O. Box 1126 Blindern, N-0318 Oslo, Norway*

<sup>5</sup>*Department of Electrical & Computer Engineering, Michigan Technological University, USA*

(Received 3 December 2014; accepted 13 January 2015; published online 22 January 2015)

Sputtering has been well-developed industrially with singular ambient gases including neutral argon (Ar), oxygen (O<sub>2</sub>), hydrogen (H<sub>2</sub>) and nitrogen (N<sub>2</sub>) to enhance the electrical and optical performances of indium tin oxide (ITO) films. Recent preliminary investigation into the use of combined ambient gases such as an Ar+O<sub>2</sub>+H<sub>2</sub> ambient mixture, which was suitable for producing high-quality (low sheet resistance and high optical transmittance) of ITO films. To build on this promising preliminary work and develop deeper insight into the effect of ambient atmospheres on ITO film growth, this study provides a more detailed investigation of the effects of ambient combinations of Ar, O<sub>2</sub>, H<sub>2</sub> on sputtered ITO films. Thin films of ITO were deposited on glass substrates by DC magnetron sputtering using three different ambient combinations: Ar, Ar+O<sub>2</sub> and Ar+O<sub>2</sub>+H<sub>2</sub>. The structural, electrical and optical properties of the three ambient sputtered ITO films were systematically characterized by X-ray diffraction (XRD), atomic force microscopy (AFM), scanning electron microscopy (SEM), Raman spectroscopy, four probe electrical conductivity and optical spectroscopy. The XRD and Raman studies confirmed the cubic indium oxide structure, which is polycrystalline at room temperature for all the samples. AFM shows the minimum surface roughness of 2.7 nm for Ar+O<sub>2</sub>+H<sub>2</sub> sputtered thin film material. The thickness of the films was determined by the cross sectional SEM analysis and its thickness was varied from 920 to 817 nm. The columnar growth of ITO films was also discussed here. The electrical and optical measurements of Ar+O<sub>2</sub>+H<sub>2</sub> ambient combinations shows a decreased sheet resistance (5.06 ohm/□) and increased optical transmittance (69%) than other samples. The refractive index and packing density of the films were projected using optical transmission spectrum. From the observed results the Ar+O<sub>2</sub>+H<sub>2</sub> ambient is a good choice to enhance the total optoelectronic properties of the ITO films. The improved electrical and optical properties of ITO films with respect to the Ar+O<sub>2</sub>+H<sub>2</sub> ambient sample were discussed in detail. In addition, the physical properties were also discussed with the influence of this ambient combination with respect to Ar, Ar+O<sub>2</sub> and Ar+O<sub>2</sub>+H<sub>2</sub>. © 2015 Author(s). All article content, except where otherwise noted, is licensed under a Creative Commons Attribution 3.0 Unported License. [<http://dx.doi.org/10.1063/1.4906566>]

<sup>a</sup>Contact authors: [pearce@mtu.edu](mailto:pearce@mtu.edu), [jeyanthinath@yahoo.co.in](mailto:jeyanthinath@yahoo.co.in)



## I. INTRODUCTION

The outstanding electrical and optical properties of transparent conducting oxides (TCOs) have been extensively studied.<sup>1</sup> For several decades, TCOs have been used in an array of applications including: flat panel displays, liquid crystal displays, plasma display panel, organic light emitting diodes, thin film transistors, solar photovoltaic (PV) cells and other optoelectronic devices.<sup>1,2</sup> TCOs are playing an important role in the enhancement of the hetero junction silicon solar cell energy conversion efficiencies.<sup>3</sup> In this particular application, the optimal characteristics are found when minimizing sheet resistance and maximizing optical transmittance.<sup>4</sup> Established TCOs are used as a transparent electrodes and window layers in PV applications including aluminium (Al)-doped zinc oxide (ZnO) or (AZO), gallium (Ga)-doped zinc oxide (ZnO) or (GZO) fluorine-doped tin oxide (SnO<sub>2</sub>) or (FTO) and tin(Sn)-doped indium oxides (ITO).<sup>5,6</sup> ITO is often the preferred material for the solar cell applications due the material's excellent electrical and optical properties. ITO is an n-type semiconductor with direct band gap of 3.5-4.3 eV.<sup>7</sup> The electrical, optical, infrared reflectance, hardness and chemical stability material properties of ITO are well characterized.<sup>8-10</sup> ITO can be fabricated by DC and RF magnetron sputtering,<sup>1,5</sup> electron beam evaporation,<sup>9</sup> thermal evaporation,<sup>11</sup> spray pyrolysis,<sup>12</sup> chemical solution deposition,<sup>13</sup> and the sol gel method.<sup>14</sup> Among the various methods, magnetron sputtering is most often used by industry to fabricate commercial optoelectronic devices.<sup>15</sup> Magnetron sputtering enables control of the electrical and optical properties of the films through different process parameters such as sputtering pressure, sputtering power, substrate temperature, discharge voltage and ambient gases.<sup>15,16</sup> Among these parameters, the ambient gases are important parameters that determine the electrical and optical properties of the ITO films, but have only been given only precursory evaluation in the literature.

Sputtering has been reported with singular ambient gases including neutral argon (Ar), oxygen (O<sub>2</sub>), hydrogen (H<sub>2</sub>) and nitrogen (N<sub>2</sub>) to enhance the electrical and optical performances of the ITO films.<sup>11,15,16</sup> Normally the ITO films are sputtered with O<sub>2</sub> ambient and annealed at H<sub>2</sub> ambient to enhance the surplus oxygen in the ITO films. The oxygen vacancies (and thus oxygen concentration) are believed to be responsible for the lowering resistivity and increasing optical transmittance in the ITO films.<sup>18,19</sup> The enhancement of oxygen concentrations in ITO films is a challenging process for the researchers and only a few reports were available for the preparation of ITO films sputtered with different ambient combinations (e.g. Ar with two reactive gases). For example, initial reports provided a preliminary investigation into the use of an Ar+O<sub>2</sub>+H<sub>2</sub> ambient mixture, which was suitable for producing high-quality (lowest sheet resistance and high optical transmittance) of ITO films.<sup>15,17</sup>

To build on this promising preliminary work and develop deeper insight into the effect of ambient atmospheres on ITO film growth, this study provides a more detailed investigation of the effects of ambient combinations of Ar, O<sub>2</sub>, H<sub>2</sub> on sputtered ITO films. Magnetron sputtered ITO films are deposited under the Ar, Ar with O<sub>2</sub>, and Ar with O<sub>2</sub> and H<sub>2</sub> (oxy-hydrogen) ambient combinations and characterized for structural, electrical and optical properties. A correlation is performed between the electrical and optical properties of ITO films results which were presented and discussed in detail to gain an understanding of the material growth and how it is influenced by different ambient combinations.

## II. EXPERIMENTAL DETAILS

### A. Thin film deposition

ITO was deposited as films on VWR Corning glass substrates by industrial designed DC magnetron sputtering unit at room temperature (20°C). The substrates were pre-cleaned using methanol and DI- water in the ultrasonic bath and dried in compressed air, before introducing them into the vacuum chamber. The base pressure of the sputtering chamber was kept in the order of 10<sup>-7</sup> mbar and during the sputtering process the pressure was maintained at 3.1x10<sup>-3</sup> mbar. The distance between the target and substrates were fixed at 8 cm and oscillation velocity was maintained at 1.2 cm/sec with a sputtering rate of 85 nm per oscillations. The working gases (e.g. Ar, O<sub>2</sub>, H<sub>2</sub>) were used for the sputtering of ITO films and commercial ITO target with the composition of 10 wt% Sn and 90%

$\text{In}_2\text{O}_3$  were used. In this study, three different ITO materials were prepared with different working gases: (1) Ar only, (2) Ar+ $\text{O}_2$ , and (3) Ar+ $\text{O}_2$ + $\text{H}_2$ . For all the cases the flow of Ar was maintained constant at 18 sccm and for the respective cases the  $\text{O}_2$  and  $\text{H}_2$  was fixed at 1 sccm in addition to Ar. The experiments were repeated three times to ensure the reproducibility of sputtered film properties.

## B. Thin-Film Characterization

The deposited ITO films were characterized for structure using X-ray diffraction (XRD) with a RIGAKU Smart Lab XRD. The surface roughness of the films was quantified using atomic force microscopy (AFM) with a JEOL JSPM-5200TM. A cross sectional view of the films was taken from scanning electron microscope (SEM) (SEM-FEI Quanta 200 FEG-ESEM). The Raman (JASCO NRS-3300) analysis was performed to study the local vibrational modes present in the samples. Optical transmittance of the films was examined from UV-visible spectrometer (Shimadzu-UV-vis) and the sheet resistance of the samples was studied using four probe resistivity method (Ai-Alessi) at room temperature and the values taken from the different locations of the films.

## III. RESULTS AND DISCUSSION

The structural properties of the deposited ITO films determined by XRD results are shown in the Fig. 1. The three main peaks (222), (400) and (440) were observed for all samples. The first two correspond to (222) and (400) planes. These observed diffraction lines agree with cubic bixbyite indium oxide structure JCPDS card No: 06-0416 and Ia-3 space group (Number: 206). Impurity of Sn phases is not observed in the XRD spectrum of any of the samples and all the deposited films show good crystalline nature at room temperature. It is evident from these results that the Sn atoms occupy the substitution sites of the indium atoms.<sup>7</sup> This indicates the different ambient combinations sputtered ITO films are in the pure form and no other phases are observed in the XRD pattern. Film (1) deposited under Ar ambient exhibited the (400) plane, while the addition of Ar+ $\text{O}_2$  in film (2) has changed its preferential orientation along (400) into (222). For film (3) Ar+ $\text{O}_2$ + $\text{H}_2$  the orientation is changed from (222) to (400). The observed diffraction lines for film (3) Ar+ $\text{O}_2$ + $\text{H}_2$  which were indexed for this ambient also reduce the crystalline nature of the ITO films. The oxygen diffusion and effusion process was performed by different ambient combinations in the sputter chamber. Luo et al. have reported that the oxygen vacancies were preferential to occupy the (400) plane and the (222) plane was well stabilized structure, so it cannot accommodate the oxygen vacancies.<sup>29</sup> Here the results indicate that the Ar and Ar+ $\text{O}_2$ + $\text{H}_2$  ambient can reduce the oxygen atoms and increase the oxygen vacancies and thus enhanced the (400) reflection. This was reflected in the position of the diffraction line shown in the XRD spectrum in Fig. 1(A). The Ar+ $\text{O}_2$ + $\text{H}_2$  ambient suppresses the intensity of the (400) plane and increases the full width half maximum (FWHM) of the (222) plane

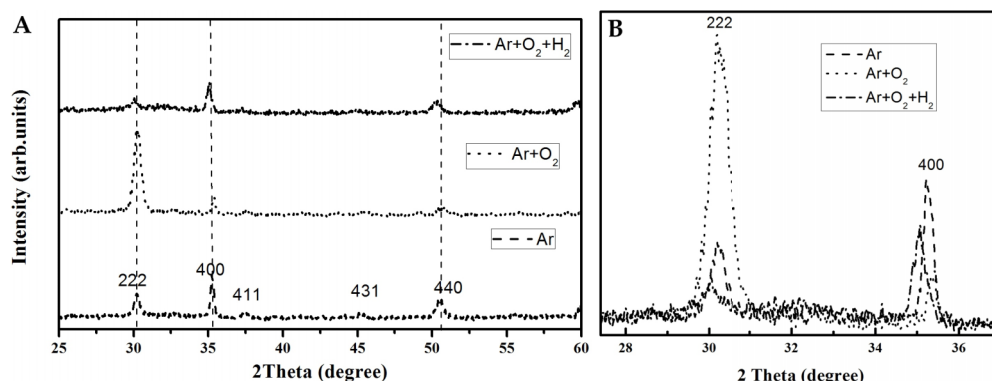


FIG. 1. (A) XRD pattern for ITO films deposited under three ambient combinations: Ar, Ar+ $\text{O}_2$  and Ar+ $\text{O}_2$ + $\text{H}_2$  (B) XRD patterns of ITO samples with the diffraction angle ( $2\theta$ ) in the range  $28^\circ$  to  $36^\circ$ .



TABLE I. Structural parameters of ITO sputtered films with Ar, Ar+O<sub>2</sub> and Ar+O<sub>2</sub>+H<sub>2</sub> ambient conditions.

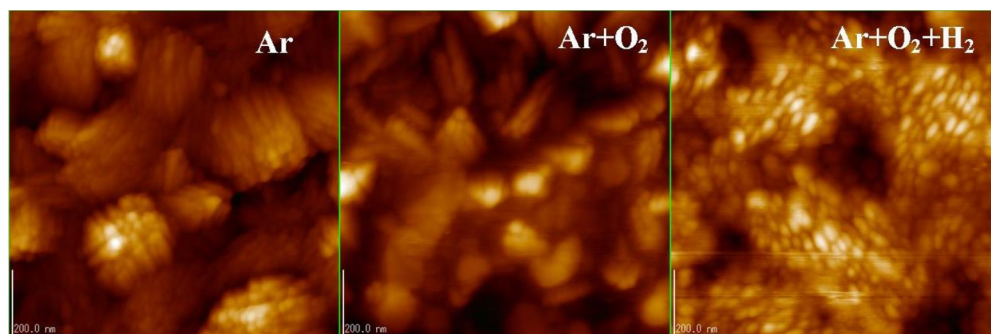
Sputtering Ambient	Preferential Orientation	d(222) Å	d(400) Å	Lattice Constant Å (222)	(400) Å	$\Delta d/d_o$ (222)	$I_{222}/I_{400}$	Grain Size in nm
	<b>Standard</b>	<b>2.9210</b>	<b>2.5290</b>	<b>10.118</b>		....	<b>3.33</b>	...
.....	.....	....	.....	.....	.....	....	....	...
<b>Ar</b>	<100>	2.9536	2.5422	10.232	10.168	0.0112	0.5714	18
<b>Ar+O<sub>2</sub></b>	<111>	2.9506	2.5352	10.221	10.140	0.0101	6.8020	28
<b>Ar+O<sub>2</sub>+H<sub>2</sub></b>	<100>	2.9289	2.5565	10.146	10.226	0.0027	1.1399	20

shown in the Fig 1(A). The grain size values were estimated using Scherrer formula and presented in Table I. The grain size values are 28 nm and 20 nm for the sample Ar+O<sub>2</sub> and Ar+O<sub>2</sub>+H<sub>2</sub> ambient, respectively. This indicates the addition of O<sub>2</sub> with H<sub>2</sub> ambient can extract the oxygen atoms from indium oxide lattices and increase the oxygen vacancies. It decreases the lattice constant and grain size value of the Ar+O<sub>2</sub>+H<sub>2</sub> deposited film.

The grain size variation is also reflected in the AFM results shown in the Fig. 2. The physical natures (grain size) of the films were strongly dependent on the different ambient combinations as was the orientation of the crystals as shown by XRD. These results support the hypothesis that the presence of hydrogen atoms occupying the indium oxide lattice in the film sample with all three gases. This shows the depression and enhancement of the (222) and (400) orientations. The other structural parameters for the three materials are summarized in the Table I. As can be seen in Table I, the different ambient combinations do not change the cubic structure, but increases or decreases the oxygen concentrations in the ITO film.

Among these parameters, the lattice constant was one of the important parameter used to explain the lattice expansions of the ITO thin films listed in Table I, was determined using the formula employed by Malathy *et al.*<sup>7</sup> Variation in the lattice constant for all the samples was calculated by the  $\Delta a = a - 10.118$ .<sup>7</sup> The  $\Delta a$  value was positive for all the samples, which shows a strong confirmation for the lattice expansions in the ITO films. These results are supported by those reported by Malathy *et al.*<sup>7</sup> and Zhang *et al.*<sup>17</sup> Compared to the sample Ar and Ar+O<sub>2</sub>, the lattice constant of the three-gas sample film was decreased, which provides additional evidence that the hydrogen atoms were positioned in the indium oxide lattice. It confirmed the decrement was due to the presence of hydrogen atoms in the ITO films. It reflected that, the Ar+O<sub>2</sub>+H<sub>2</sub> ambient produced the large amount of oxygen vacancies in the ITO films compared to the other ambient conditions.

The intensity ratios ( $I_{222}/I_{400}$ ), for the materials with Ar, Ar+O<sub>2</sub> and Ar+O<sub>2</sub>+H<sub>2</sub> ambient conditions had values of 0.5714, 6.8020 and 1.1399, respectively (Fig. 1(B)). By comparing the results with intensity ratio of bulk indium oxide (3.33), the high and low intensity ratios were observed for all of the materials. In general, the intensities ratio was responsible for the combination of In<sup>3+</sup> and O<sup>2-</sup> ions in the ITO films.<sup>20</sup> This kind of pairing enhances the indium oxide network formation and maintain the periodicity of the indium oxide. A critical level of In<sup>3+</sup> and O<sup>2-</sup> pairs are required for the

FIG. 2. Surface topography image for 200 nm x 200 nm of the ITO film samples under ambient Ar, Ar+O<sub>2</sub> and Ar+O<sub>2</sub>+H<sub>2</sub>.

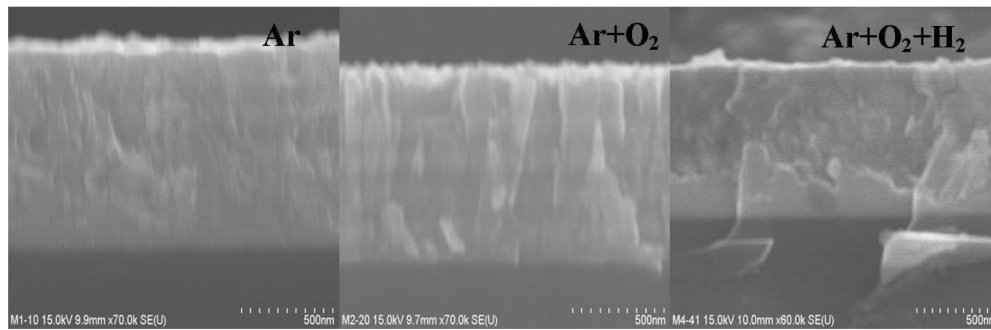


FIG. 3. Cross sectional scanning electron microscopy image of the film deposited under Ar, Ar+O<sub>2</sub> and Ar+O<sub>2</sub>+H<sub>2</sub>.

formation. Below the critical level defects in the indium oxide films will result. Hence the intensity of the films was changed with respect to these combinations, which are reflected in the XRD spectra. The intensity of the plane will change with respect to the oxygen concentrations in the ITO films. In the results presented here, the Ar+O<sub>2</sub>+H<sub>2</sub> ambient combination reduces the oxygen concentrations in the (222) plane and increase the oxygen vacancies. Thus, it suppresses the intensity of the (222) plane and stimulate the (400) orientation of the ITO films. This result was clearly exhibited in the intensity ratio values. Compared to the intensity ratio of the Ar-only film, the Ar+O<sub>2</sub>+H<sub>2</sub> ambient film is slightly higher indicating that this ambient may conserve the oxygen concentrations in the ITO films compared to the Ar ambient sputtered film. This suppresses the oxidation nature of the ITO films and was highly oriented along the (400) reflection. This affects the columnar growth of the ITO film for the sample Ar+O<sub>2</sub>+H<sub>2</sub> ambient film (shown in the Fig. 3) and spherical shape grains were observed (shown in the Fig. 2).

Fig. 2 shows the AFM images of the ITO sputtered films. Roughness values were taken from the area of 200 x 200 nm. As can be seen in Fig. 2 there was a change in the surface morphology of the samples with the addition of different ambient combinations. The root means square (rms) surface roughness of 10.9, 12.9 and 2.70 nm for the Ar, Ar+O<sub>2</sub> and Ar+O<sub>2</sub>+H<sub>2</sub> ambient conditions samples was observed respectively. The least surface roughness of 2.7 nm is observed for ITO sputtered with Ar+O<sub>2</sub>+H<sub>2</sub> combinations.

The Ar only sample does not contain any other pin holes and spikes. In the presence of Ar with O<sub>2</sub> ambient, the grains were changed into a prismatic shape. Then, the prismatic grains were changed into spherical shape under the Ar+O<sub>2</sub>+H<sub>2</sub> ambient combinations. These types of fine grains reduce the surface roughness values of the Ar+O<sub>2</sub>+H<sub>2</sub> atmosphere film and enhance the electrical conductivity (shown in the Table II). These types of changes were observed in the XRD, electrical and optical results. Normally the Ar+O<sub>2</sub> ambient enhance the oxidation nature and change its preferential orientation of the ITO film (shown in the XRD results). The surface roughness (12.9 nm) for the film deposited with Ar+O<sub>2</sub> combination is increased in agreement with Sungthong *et al.*<sup>21</sup> The oxygen ambient leads to increase void fraction in the Ar with oxygen ambient sputtered ITO film and as shown here increase the surface roughness of the films.

The addition of hydrogen ambient can play a major role in to enhance the surface properties of the ITO films. However, here the Ar+O<sub>2</sub>+H<sub>2</sub> sample has attained smoother surface compared to the other respective samples and this ambient combinations decrease the oxygen concentrations and

TABLE II. Electrical and optical parameters of ITO films with Ar, Ar+O<sub>2</sub> and Ar+O<sub>2</sub>+H<sub>2</sub> ambient conditions.

Sputtering Ambient	Thickness nm	UV Transmittance (400-800 nm)	Band gap (eV)	Sheet Resistance Ω/□	Resistivity x10 <sup>-4</sup> Ω-cm	Packing Density
<b>Ar</b>	920	52%	3.56	7.14	6.57	0.9465
<b>Ar+O<sub>2</sub></b>	880	86%	3.48	105.76	93.07	0.9107
<b>Ar+O<sub>2</sub>+H<sub>2</sub></b>	817	69%	3.55	5.06	4.13	0.8966



increase the oxygen vacancies. Here, the addition of Ar+O<sub>2</sub>+H<sub>2</sub> ambient suppress the oxidation nature and enhance the oxygen vacancies. So, the least surface roughness was responsible for the decrement of sheet resistance (105.76 to 5.06  $\Omega/\square$ ) of the Ar+O<sub>2</sub>+H<sub>2</sub> film. This type of insufficient oxidation can decrease the film thickness of the film Ar+O<sub>2</sub>+H<sub>2</sub>. But this combination may produce the H<sub>2</sub>O molecules which produce the pin holes in the surface of the Ar+O<sub>2</sub>+H<sub>2</sub> film.

Fig. 3 shows the cross sectional view of the SEM images of the ITO sputtered with different ambient combinations. Film thickness of the ITO films was varied from 920 to 817 nm as shown in Table II. The minimum thickness was observed for the sample with Ar+O<sub>2</sub>+H<sub>2</sub> ambient. Particularly this ambient can induce the insufficient oxidation and it may extract the oxygen atoms from the surface of the ITO films. It was caused by oxygen release and surface decomposition of the ITO film.<sup>5</sup> So it reduces the oxygen concentrations in the ITO films. Hence the film thickness is reduced compared to other samples.

In this cross section SEM images, the microstructural changes were observed for the different ambient combination sputtered ITO films. These changes were reflected in the structural, electrical and optical results. Initially, the columnar grain growth was observed in the Ar-only sample and the Ar+O<sub>2</sub> sample shown in the Fig. 3. These results clarify that, once nucleation growth is formed on the glass substrate further crystallites grow continuously under the Ar and Ar+O<sub>2</sub> ambient conditions. These ambient combinations are responsible for the columnar growth nature of the ITO films. In these two ambient combinations sputtered films, the higher surface roughness values are observed. The Ar+O<sub>2</sub> ambient film has shown the highest roughness value (12.8 nm). With the addition of excess oxygen, the roughness of the ITO film increases. The Ar+O<sub>2</sub>+H<sub>2</sub> ambient could distort the columnar growth of the ITO films represented in the Fig. 3 and decrease the roughness value. The growth distortion was exhibited in the XRD spectrum for the Ar+O<sub>2</sub>+H<sub>2</sub> sample. But the minimum surface values decrease the sheet resistance of the ITO films. The Ar+O<sub>2</sub>+H<sub>2</sub> ambient increases the hydroxyl bonds (-OH) thus creating the dangling bonds in the ITO films. The AFM images for the Ar+O<sub>2</sub>+H<sub>2</sub> materials show the pin holes and it was an evidence for the hydroxyl bond (-OH) formed under the Ar+O<sub>2</sub>+H<sub>2</sub> ambient combinations. It also made effects the In-O bonding network formation for further film growth. So, the inhomogeneity was increased and it suppresses the nucleation growth of the ITO film. Because the suppression of the film growth strongly depends on the number of hydroxyl bonds formed in the ITO films. Ando et al. have observed the similar trends in ITO sputtered with H<sub>2</sub> O additions.<sup>22</sup> An addition of oxy-hydrogen nature induces the formation of oxygen vacancies in the ITO films. In the present work, the selected hydrogen ambient ratio is 1- sccm. Compared to the other reports, this study used a higher hydrogen ratio, so it may be a possible reason for the production of large number of hydroxyl bonds in the ITO films. This type of inhomogeneity affects the crystalline nature and columnar growth of the ITO film Ar+O<sub>2</sub>+H<sub>2</sub> sample. So, it decreases the surface roughness of the films, which is compared to the other respective samples.

The structural conformation of the ITO films was determined with Raman spectroscopy and the corresponding spectra are shown in Fig 4. According to the structure factor of group analysis the indium oxide 4A<sub>g</sub> (Raman) +4E<sub>g</sub> (Raman) +14T<sub>g</sub> (Raman) +5A<sub>u</sub> (inactive) +16T<sub>u</sub> (infrared) modes are predicted.<sup>23</sup> The observed corresponding modes agreed with the reported cubic indium oxide structure. For Ar ambient sputtered film, the modes were observed as 305 (E<sub>g</sub>), 362 (E<sub>g</sub>-external), 499 and 555 (A<sub>1g</sub>). In the Ar+O<sub>2</sub> ambient films have attained film 302 (E<sub>g</sub>) and 548 (A<sub>1g</sub>). The Ar+O<sub>2</sub>+H<sub>2</sub> ambient sputtered film had modes at 313 and 359 cm<sup>-1</sup>.<sup>24</sup> A noticeable broad peak is observed at 1103 cm<sup>-1</sup> for Ar ambient sputtered materials. Similarly, the Ar+O<sub>2</sub> and Ar+O<sub>2</sub>+H<sub>2</sub> ambient sputtered materials peak was observed at 1090 cm<sup>-1</sup>. These corresponding peaks were detected for commercially sputtered ITO films.<sup>25</sup> The observed corresponding modes agreed with the XRD results of cubic indium tin oxide. The other mixed phases were not observed in the Raman spectra indicating that the different ambient combinations do not change its structure. This is additional evidence that different ambient combinations do not change the structure of the ITO films.

The electrical properties of the deposited ITO films are examined by the four point probe resistivity measurements. The sheet resistance values are 7.14, 105.76 and 5.06  $\Omega/\square$  for Ar, Ar+O<sub>2</sub> and Ar+O<sub>2</sub>+H<sub>2</sub> ambient conditions, respectively. The obtained sheet resistance values of the oxy-hydrogen ambient sputtered films showed the lowest sheet resistance (5.06  $\Omega/\square$ ). In the Ar ambient sputtered films, Ar neutral bombardments create the Si dangling bonds in the glass substrate. These dangling

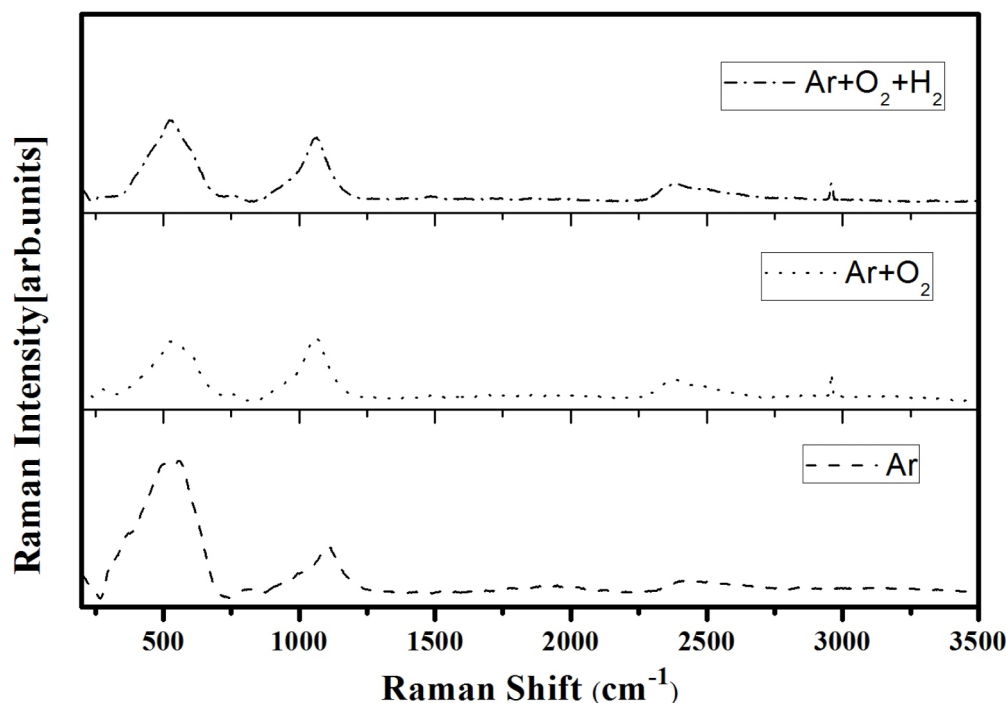


FIG. 4. Raman spectra for the ITO films deposited under ambient Ar, Ar+O<sub>2</sub> and Ar+O<sub>2</sub>+H<sub>2</sub>.

bonds extract the oxygen atoms in the growing ITO film and creates the oxygen vacancies in the ITO film.<sup>26</sup> So, the Ar ambient nature has significantly increased the oxygen vacancies and reduced the sheet resistance value close to the Ar+O<sub>2</sub>+H<sub>2</sub> ambient condition film. Another factor responsible for the large number of vacant sites in the Ar+O<sub>2</sub>+H<sub>2</sub> ambient sputtered ITO film. It is due to the absence of oxygen gas in the sputtering chamber. Similarly the simultaneous flow of oxygen with hydrogen gases in the sputter chamber produces oxygen vacancies. The hydrogen atoms occupy the oxygen sites in the indium oxide lattice and reduce the oxygen concentrations. Generally, the oxygen vacancies gave two additional electrons for the conduction of ITO films.<sup>27</sup> In addition to that the hydrogen atoms also release one electron for its conduction. Hence, the oxygen vacancies and hydrogen atoms play an important role in the decrement of sheet resistance of the ITO films. This is clearly shown in the sudden decrement of sheet resistance values from 105.76 to 5.06 Ω/□. Compared to the Ar+O<sub>2</sub> combination nature, the Ar+O<sub>2</sub>+H<sub>2</sub> is favourable for the enhancement of electrical resistivity of the ITO films. Okada, et al. reported that the denser oxygen vacancies or richest hydrogen atoms are responsible for the lowest sheet resistance in the ITO film.<sup>18</sup> The oxygen with hydrogen ambient is suitable for reducing the oxygen concentration in the ITO film under Ar+O<sub>2</sub>+H<sub>2</sub> ambient conditions.

Fig. 5(A) shows the transmittance spectra recorded for the ITO films sputtered with different ambient combinations. The average transmittance was measured in the visible region (400-800 nm) for all the samples. The oscillation observed in the transmittance spectra was due to the difference in the index of refraction between the substrate and film thickness.<sup>28</sup> Here, the observed transmittance values lie between 52%-86%. From the transmittance results, the Ar+O<sub>2</sub> ambient sputtered film exhibits the highest average transmittance of ~86%. It was due to the largest grain size of the film (28 nm) with reduced grain boundary scattering which enhances the transmittance properties.<sup>17</sup> The results indicate that the oxygen ambient is suitable for enhancement of the transmittance property of the ITO films. The transmittance of Ar+O<sub>2</sub>+H<sub>2</sub> (69%) sample was increased when compared to the Ar ambient sputtered film. With the addition of oxygen with hydrogen ambient; increase in the transmittance and decrease in the sheet resistance of the ITO films was observed. The addition of Ar+H<sub>2</sub> ambient increased the oxygen vacancies and decreased the oxygen concentrations in the ITO films. It induces more metallic nature of the ITO films.<sup>29</sup> However, in this case, the addition of Ar with oxygen and hydrogen ambient nature maintains the oxygen levels in the ITO films and slightly

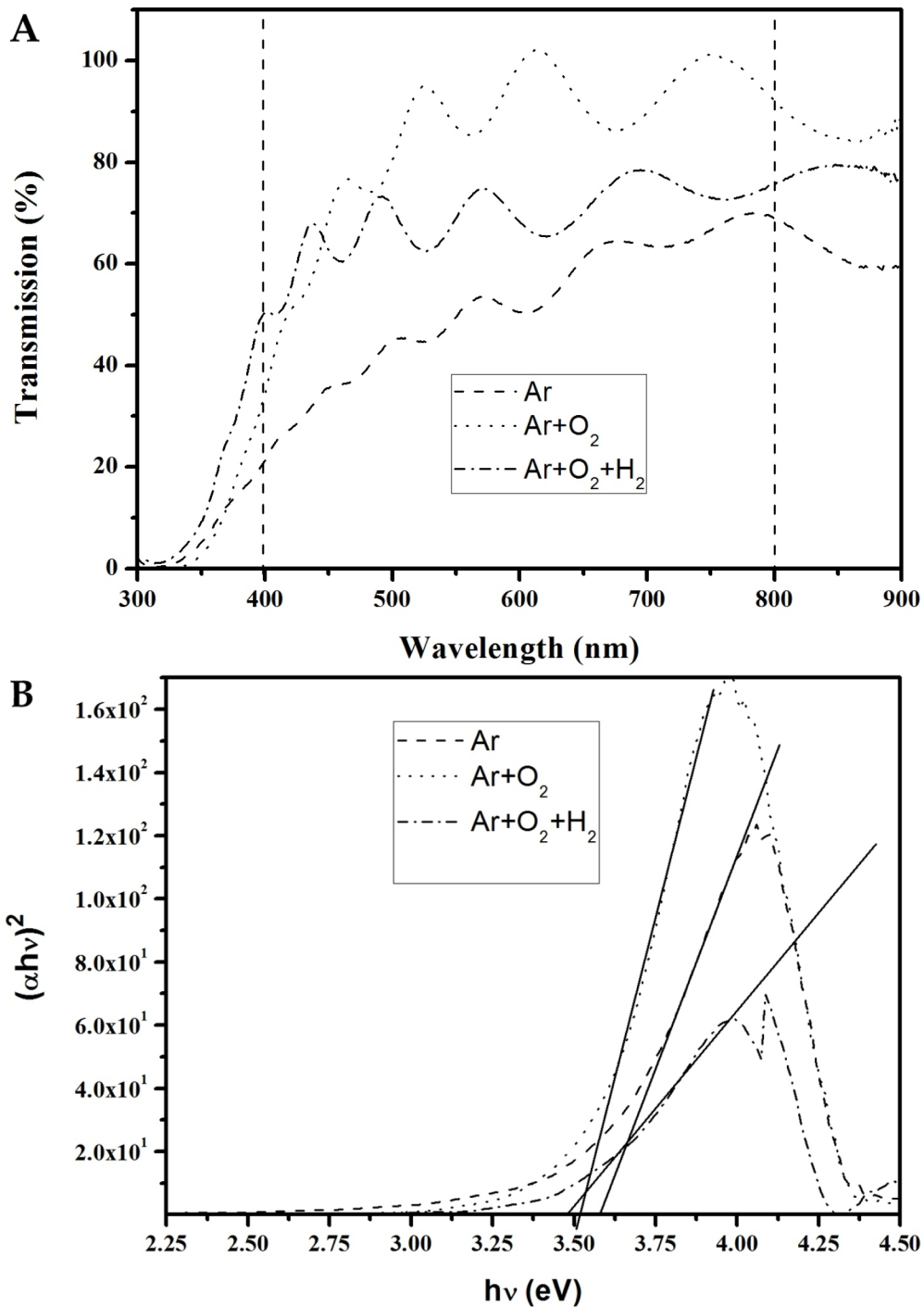


FIG. 5. (A) Optical transmission spectrum for the ITO sputtered with three different ambient combinations (B) Tauc plot of samples ITO films deposited under ambient Ar, Ar+O<sub>2</sub> and Ar+O<sub>2</sub>+H<sub>2</sub>.

increases the transmittance value. All the transmittance results showed, the Ar with oxygen ambient may increase the transmittance nature of the ITO films. Das, et al. also observed the transmittance of the films increased in the oxygen ambient sputtered film.<sup>30</sup>

The refractive indexes of the films were the important parameter to realize the optical performances of the ITO films. The refractive index was estimated with the Swanepoel envelop method

using transmittance spectrum in the visible region (using the transmittance maximum and minimum value for the corresponding wavelength) for all the samples.<sup>31</sup> The refractive index of the films changed from 2.01, 1.95 and 2.07 for the Ar, Ar+O<sub>2</sub> and Ar+O<sub>2</sub>+H<sub>2</sub> ambient condition samples respectively. The high crystalline nature of the Ar+O<sub>2</sub> condition shows the minimum index values. The high crystalline nature can improve the transmittance property of the ITO films. The film packing density was indicated by the Clausius-Mossotti relation.<sup>32</sup> In this relation, the packing density of the films can be estimated by the respective refractive index. Film density varied for each sample as is summarized in Table II.

Moss also derived the relation between band gap and refractive index of the semiconducting materials.<sup>33</sup> Kumar, et al. reported the modified Moss relation and reported that the estimated index values closely match experimental values.<sup>34</sup> These above mentioned two methods based on the refractive index values closely match with reported values (measured from ellipsometry).<sup>35</sup>

The absorption edges of the films were varied as the function of different ambient combinations. The higher (red) and lower (blue) wavelength shift observed for three different ambient sputtered ITO films. The absorption edge represents the electron transition between the valance band to conduction band, i.e. band gap. The optical transmittance spectrum was used to estimate the optical band gap of the respective material. From the transmittance spectra, the optical band gap of the ITO films was determined by the following equation.

$$\alpha h\nu = A(h\nu - E_{\text{opt}})^N \quad (1)$$

Where N is the transition probability,  $h\nu$  is the photon energy,  $E_{\text{opt}}$  is the optical band gap and A indicates the allowed transitions. N represents the different transitions such as direct, allowed indirect, forbidden direct, forbidden indirect with the values 1/2, 2, 3/2 and 3 respectively. The optical band gap was evaluated from  $(\alpha h\nu)^2$  vs  $h\nu$  plot for all the films shown in the Fig 5 (B). The obtained band gap values 3.56, 3.48 and 3.55 eV for sample Ar, Ar+O<sub>2</sub> and Ar+O<sub>2</sub>+H<sub>2</sub> ambient condition, respectively. The observed band gap is in agreement with previous reported values.<sup>7</sup> The variations in the optical band gap were explained by Burstein-Moss shift.<sup>36</sup> Generally in a degenerate semiconductor the optical band gap increases or decreases by varying the carrier concentrations in the ITO films. Here the Ar+O<sub>2</sub> ambient films exhibited the lowest band gap, ie. Larger grain size and high crystalline nature may reduce the oxygen vacancies. Leenheer, et al. observed decrease in the indium zinc oxide band gap with addition of oxygen gas.<sup>37</sup> It may decrease the carrier concentration and increase the resistivity of the ITO films (Ar+O<sub>2</sub>). But the sample Ar and Ar+O<sub>2</sub>+H<sub>2</sub> exhibited the denser oxygen vacancies and smaller grain size which can increase the optical band gap. So it exhibits the lowest sheet resistance values for the film Ar and Ar+O<sub>2</sub>+H<sub>2</sub>.

The greater understanding of ITO materials that these results provided are promising and indicate that future work is needed to optimize ITO films using different oxygen and hydrogen gas mixtures. These films can then be annealed under various ambient conditions to further enhance the electrical and optical properties of the ITO films for solar cell applications. In addition, investigating the prepared samples on silicon and silicon dioxide substrates will provide further insights into the ITO properties by reducing the oxygen concentration to improve conductivity and transmission of the ITO films towards optoelectronic devices. These optimized films can be used for the fabrication of thin film a-Si:H heterojunction solar cells with enhanced efficiency and low cost.

#### IV. CONCLUSIONS

This study investigated the deposition of ITO on glass substrates by DC magnetron sputtering using three different ambient combinations. The structural, electrical and optical properties of the ITO films were studied in detail with respect to the different ambient combinations to gain a better fundamental understanding of ITO growth and were shown to have a significant impact on the properties of the films. The results show that the electrical and optical properties of the ITO films were improved using the Ar+O<sub>2</sub>+H<sub>2</sub> ambient conditions. The Ar+O<sub>2</sub>+H<sub>2</sub> film has a reduced sheet resistance and a moderate optical transmission when compared to the other two different ambient sputtered samples. Hence, from all the analysis we conclude that the three gas ambient sputtered ITO film exhibited superior optoelectronic properties. So this ambient combination may possibly favourable for enhancing

the optoelectrical properties of the ITO films. In future, the optimized level of the gas compositions leads to the preparation of suitable films for optoelectronic devices. These results are promising and indicate that improved ITO films can be fabricated for solar photovoltaic applications using a tri-gas ambient during magnetron sputtering.

## ACKNOWLEDGMENTS

The authors are thankful to the DST-SERB/F/1829/2012-2013 for partial support. JM thanks the UGC for providing support through RAMAN fellowship 2014-2015 to visit Michigan Technological University, USA. The authors would like to thank Mr. V. Ragavendran for his assistance, Dr. Smagul Karazhanov, Senior scientist, Institute for Energy Technology, for helpful discussions and Dr. M.H. Rein for their valuable suggestions.

- <sup>1</sup> V. A. Dao, H. Choi, J. Heo, H. Park, K. Yoon, Y. Lee, Y. Kim, N. Lakshminarayan, and J. Yi, *Curr. Appl. Phys* **10**, S506 (2010).
- <sup>2</sup> S. K. Choi and J. Lee, *J. Vac. Sci. Technol* **5**, A19 (2001).
- <sup>3</sup> Z. Erjing, Z. Weijia, L. Jun, Y. Dongjie, H. J. Jacques, and Z. Jing, *Vacuum* **86**, 290 (2011).
- <sup>4</sup> C. Y. Wu, B. T. Lin, Y. J. Zhang, Z. Q. Li, and J. J. Lin, *Phys. Rev. B* **85**, 104204 (2012).
- <sup>5</sup> I. Hotovy, J. Pezoldt, M. Kadlecikova, T. Kups, L. Spiess, J. Breza, E. Sakalauskas, R. Goldhahn, and V. Rehacek, *Thin Solid Films* **518**, 4508 (2010).
- <sup>6</sup> S. Calnan and A. N. Tiwari, *Thin Solid Films* **518**, 1839 (2010).
- <sup>7</sup> V. Malathy, S. Sivaranjani, V. S. Vidhya, T. Balasubramanian, J. Joseph Prince, C. Sanjeeviraja, and M. Jayachandran, *J. Mater. Sci.: Mater. Electron* **21**, 1299 (2010).
- <sup>8</sup> J. M. Gaskell and D. W. Sheel, *Thin Solid Films* **520**, 4110 (2012).
- <sup>9</sup> M. Himmerlich, M. Koufaki, Ch. Mauder, G. Ecke, V. Cimalla, J. A. Schaefer, E. Aperathitis, and S. Krischok, *Surf. Sci.* **601**, 4082 (2007).
- <sup>10</sup> M. Gulen, G. Yildirim, S. Bal, A. Varilci, I. Belenli, and M. Oz, *J. Mater. Sci.: Mater. Electron* **23**, 928 (2012).
- <sup>11</sup> V. Vasu and A. Subrahmanyam, *Semicond. Sci. Technol* **7**, 320 (1992).
- <sup>12</sup> M. Nisha, S. Anusha, A. Antony, R. Manoj, and M. K. Jeyaraj, *Appl. Surf. Sci* **252**, 1430 (2005).
- <sup>13</sup> J. Lee, S. Lee, G. Li, M. A. Petruska, D. C. Paine, and S. Sun, *J. Am. Chem. Soc* **134**, 13410 (2012).
- <sup>14</sup> H. Cho and Y. H. Yun, *Ceram. Int.* **27**, 615 (2011).
- <sup>15</sup> R. BelHadjTahar, T. Ban, Y. Ohya, and Y. Takahashi, *J. Appl. Phys* **83**, 5 (1998).
- <sup>16</sup> K. Kato, H. Omoto, T. Tomioka, and A. Takamatsu, *Thin Solid Films* **520**, 110 (2011).
- <sup>17</sup> K. Zhang, F. Zhu, C. H. A. Huan, and A. T. S. Wee, *J. Appl. Phys* **86**, 2 (1999).
- <sup>18</sup> K. Okada, S. Kohiki, S. Luo, D. Sekiba, S. Ishii, M. Mitome, A. Kohno, T. Tajiri, and F. Shoji, *Thin Solid Films* **519**, 3557 (2011).
- <sup>19</sup> T. Ashida, A. Miyamura, N. Oka, Y. Sato, T. Yagi, N. Taketoshi, T. Baba, and Y. Shigesato, *J. Appl. Phys* **105**, 073709 (2009).
- <sup>20</sup> Y. J. Kim, S. B. Jin, S. I. Kim, Y. S. Choi, I. S. Choi, and J. G. Han, *Thin Solid Films* **518**, 6241 (2010).
- <sup>21</sup> A. Sungthong, S. Porntheeraphat, A. Poya, and J. Nukeaw, *Appl. Surf. Sci* **254**, 7950 (2008).
- <sup>22</sup> M. Ando, E. Nishimura, K. I. Onisawa, and T. Minemura, *J. Appl. Phys* **93**, 2 (2003).
- <sup>23</sup> D. Liu, W. W. Lei, B. Zou, S. D. Yu, J. Hao, K. Wang, B. B. Liu, Q. L. Cui, and G. T. Zou, *J. Appl. Phys* **104**, 083506 (2008).
- <sup>24</sup> O. M. Berengue, A. D. Rodrigues, C. J. Dalmaschio, A. J. C. Lanfredi, E. R. Leite, and A. J. Chiquito, *J. Phys. D: Appl. Phys* **43**, 04540 (2010).
- <sup>25</sup> R. Chandrasekhar and K. L. Choy, *Thin solid films* **398**, 59 (2001).
- <sup>26</sup> S. N. Luo, A. Kono, N. Nouchi, and F. Shoji, *J. Appl. Phys* **100**, 113701 (2006).
- <sup>27</sup> R. Savu and E. Joanni, *Thin Solid Films* **515**, 7813 (2007).
- <sup>28</sup> A. J. Leenheer, J. D. Perkins, M. F. A. M. Van Hest, J. J. Berry, R. P. O. Hayre, and David S. Ginley, *Phys. Rev B* **77**, 115215 (2009).
- <sup>29</sup> S. Luo, S. Kohiki, K. Okada, F. Shoji, and T. Shishido, *Phys. Status Solidi A* **207**, 386 (2010).
- <sup>30</sup> R. Das, K. Adhikary, and S. Ray, *Appl. Surf. Sci* **253**, 6068 (2007).
- <sup>31</sup> R. Swanepoel, *J. Phys. E: Sci. Instrum* **16** (1983).
- <sup>32</sup> M. Subramanian, S. Vijayalakshmi, S. Venkataraj, and R. Jayavel, *Thin Solid Films* **516**, 3776 (2008).
- <sup>33</sup> T. S. Moss, *Proc. Phys. Soc. B* **63**, 167 (1950).
- <sup>34</sup> V. Kumar and J. K. Singh, *Indian J pure & Appl phys* **48**, 571 (2010).
- <sup>35</sup> H. Han and J. W. Mayer, *J. Appl. Phys* **100**, 083715 (2006).
- <sup>36</sup> I. Hamberg and C. G. Granqvist, *Phys. Rev. B* **30**, 6 (1984).
- <sup>37</sup> A. J. Leenheer, J. D. Perkins, M. F. A. M. Van Hest, J. J. Berry, R. P. O'Hayre, and D. S. Ginley, *Phys. Rev. B* **77**, 115215 (2008).